Available online at www.sciencedirect.com
SCIENCE DIRECT®
Journal of Photochemistry and Photobiology A: Chemistry 165 (2004) 75–89
Journal of Photochemistry and Photobiology A:Chemistry
www.elsevier.com/locate/jphotochem

Photo-degradation of bacteriochlorophyll c in intact cells and extracts from *Chlorobium tepidum*

A. Granzhan [a], A. Penzkofer [a,*], G. Hauska [b]

[a] *Institut II, Experimentelle und Angewandte Physik, Universitaet Regensburg, Universitätsstrasse 31, D-93053 Regensburg, Germany*
[b] *Institut für Botanik, Universitaet Regensburg, Universitätsstrasse 31, D-93053 Regensburg, Germany*

Received 3 October 2003; received in revised form 13 February 2004; accepted 1 March 2004

Abstract

The photo-stability of bacteriochlorophyll c (Bchlc) in an acetone–methanol–water solution extracted from *Chlorobium tepidum* and in the chlorosomes of intact *Chlorobium tepidum* cells is studied. The photo-stability of Bchlc in the chlorosomes is high (quantum yield of photo-degradation $\phi_D \approx 8 \times 10^{-7}$). In air-saturated acetone–methanol–water solution the photo-degradation of Bchlc is caused by chemical reaction with the dissolved oxygen, where triplet Bchlc produces singlet oxygen, and singlet oxygen reacts with Bchlc to form stable oxidized linear tetrapyrroles as well as intermediate oxidized bacteriochlorophylls. The intermediate photoproducts degrade to linear tetrapyrroles by the catalytic action of triplet oxygen. The initial quantum yield of photo-degradation is direct proportional to the concentration of Bchlc giving $\phi_{D,0} \approx 0.011$ for a 7×10^{-6} M solution at an excitation wavelength of 672 nm. In nitrogen-bubbled solution the photo-degradation is dominated by direct photoproduct formation in the triplet state of Bchlc. Long-wavelength absorbing intermediate photoproducts degrade slowly in the dark to short-wavelength absorbing stable photoproducts. The quantum yield of photo-degradation of a de-oxygenated solution was found to be $\phi_{D,0} \approx 0.0012$ for excitation at 672 nm.

Keywords: Bacteriochlorophyll c; *Chlorobium tepidum*; Photo-degradation; Photo-oxidation

1. Introduction

The green sulfur photosynthetic bacteria like *Chlorobium tepidum* [1–4] are obligate photoautotrophs and strict anaerobes that grow in sulfide-rich environment. They adjust to the ambient light conditions [5]. In dim light they are very efficient light converters in photosynthesis due to their light harvesting chlorosomes [1,6] which absorb light and transfer the excitation energy to the reaction center [7,8]. The chlorosomes contain rod-like aggregates made up mainly of bacteriochlorophyll c (Bchlc) molecules [9,10]. A detailed characterization of bacteriochlorophylls is found in [11–14]. The structural formula of Bchlc in two mesomeric forms is shown in Fig. 1a. The IUPAC-IUB nomenclature is used for labeling [15,16]. Bacteriochlorophyll c deprived of the magnesium ligand is called bacteriopheophytine c (Bphec).

The photo-bleaching of chlorophylls and bacteriochlorophylls is reviewed in [13,17] The photo-oxidation of magnesium-free bacteriochlorophyll c derivatives is studied in [18–21]. The triplet-state properties of Bchlc and the singlet-oxygen photo-generation and quenching in Bchlc are investigated in [22]. The singlet-oxygen formation and deactivation in photosynthetic systems is studied in [23,24].

Here we investigate the room temperature photo-stability of Bchlc bound in chlorosomes of intact *Chlorobium tepidum* cells, and of Bchlc molecules in an acetone–methanol–water solution extracted from *Chlorobium tepidum*. Quantum yields of photo-degradation of Bchlc in intact cells and in solution are determined. Some photoproducts are tried to be identified (linear tetrapyrroles, bacteriochlorophyll a-like species, bacteriochlorophyll c-like species). Studies are carried out under air-saturated conditions, and under de-aerated conditions. The degradation is studied optically by measuring time dependent transmission changes for different excitation conditions. The quantum yield of photo-degradation, ϕ_D, as defined by the number of degraded molecules to the number of absorbed photons, is determined.

The recording of absorption coefficient spectra at different times for fixed excitation wavelengths reveals the formation and degradation of photoproducts. Bchlc destruction in air-saturated solution is found to be due to (i) oxidative linear tetrapyrrole formation by ring cleavage [13,17–24]; (ii) the formation of two oxidized Bchla-like molecule

* Corresponding author. Tel.: +49-941-943-2107; fax: +49-941-943-2754.
E-mail address: alfons.penzkofer@physik.uni-regensburg.de (A. Penzkofer).

1010-6030/$ – see front matter © 2004 Elsevier B.V. All rights reserved.
doi:10.1016/j.jphotochem.2004.03.001

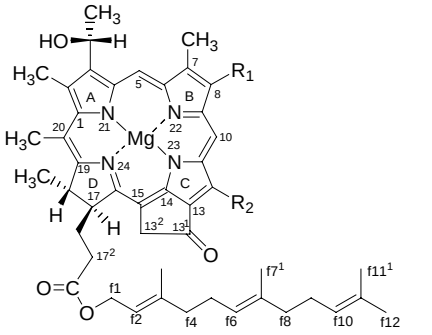

(a) Bacteriochlorophyll c

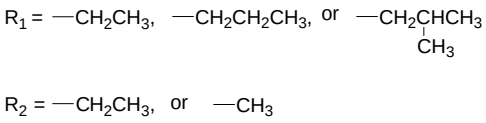

(b) Substituents

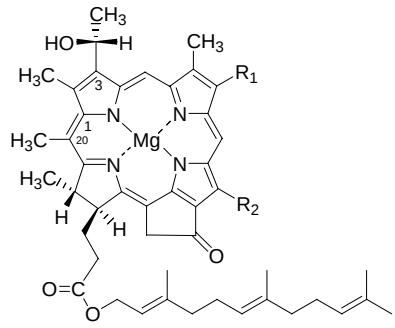

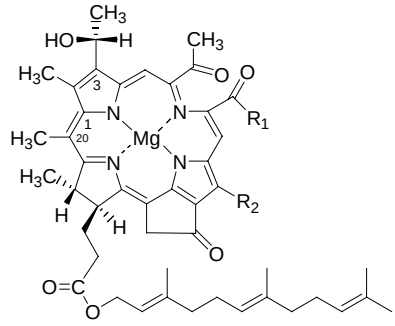

(c) Bchla-I, Bchla-II

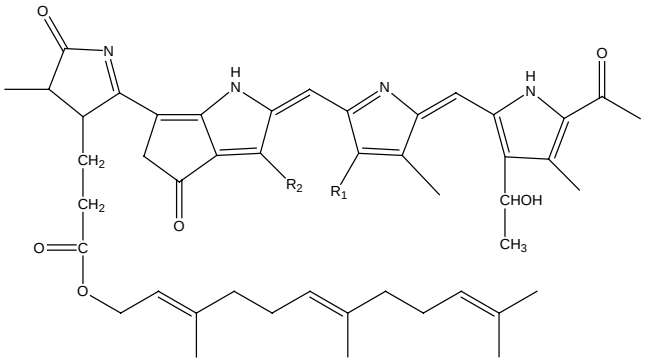

(d) linear tetrapyrrole

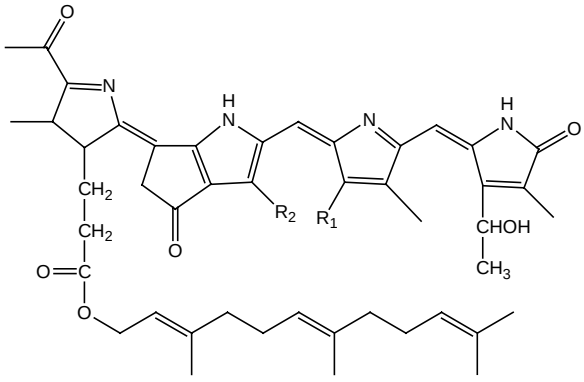

(e) linear tetrapyrrole

Fig. 1. Structural formulae: (a) two mesomeric forms of bacteriochlorophyll c (from [2,47]); (b) substituents (from [2]); (c) oxidized bacteriochlorophyll a-like structure Bchla-I and Bchla-II; (d) oxidized linear tetrapyrrole from Bchlc broken at C19–C20 position; (e) oxidized linear tetrapyrrole from Bchlc broken at C20–C1 position.

structures (called Bchla-I and Bchla-II); and (iii) the formation a Bchlc-like molecule structure (called Bchlc-I) after singlet-oxygen generation. Singlet oxygen is formed by triplet Bchlc interaction with triplet ground-state oxygen. The oxidized bacteriochlorophyll derivatives further degrade slowly in the dark by interaction with ground-state triplet oxygen. De-aerated Bchlc solutions are more stable than air-saturated Bchlc solutions. It will be shown that they mainly photo-degrade directly form the triplet-excited state to intermediate and stable photoproducts of slightly different absorption spectra.

2. Experimental

The green sulfur bacteria *Chlorobium tepidum* were grown by a procedure described in [25]. The culture was stored in a refrigerator at 4 °C before usage.

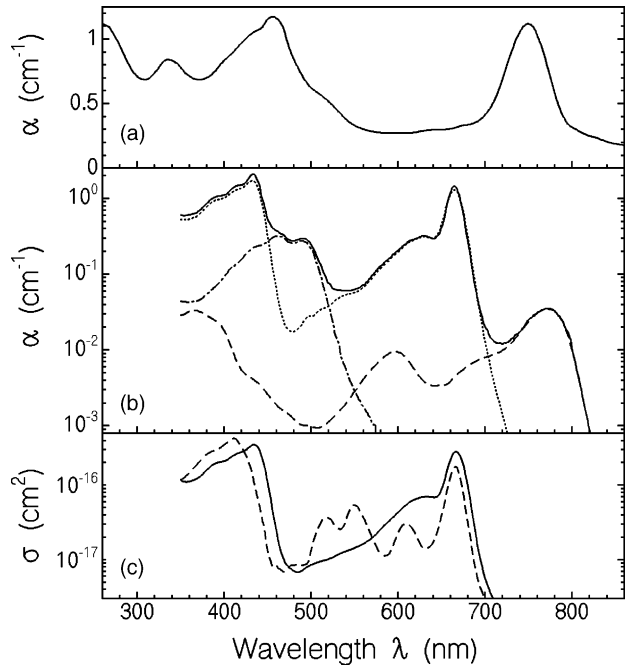

Fig. 2. (a) Absorption coefficient spectrum of *Chlorobium tepidum* cell suspension diluted in Tris-buffer a factor of 10 (see text). Concentration of Bchlc is $C_{C,0} \approx 8.8 \times 10^{-6}$ mol dm^{-3}. Scattering contribution is not removed. (b) Absorption coefficient spectrum of *Chlorobium tepidum* extract in acetone–methanol–water (7:2:1 volume ratio) solution (solid curve). Dashed curve, contribution of Bchla (shape from [28]). Dash-dotted curve, contribution from carotenoids (shape from [30]). Dotted curve, contribution of Bchlc (difference spectrum). Concentration of Bchlc is $C_{C,0} \approx 8 \times 10^{-6}$ mol dm^{-3}. (c) Absorption cross-section spectra of bacteriochlorophyll c in acetone (solid curve, from [34]) and of bacteriopheophytine c in acetone (dashed curve, from [34]).

The photo-degradation of the intact cells was studied with stock cell culture diluted 1:10 with an aqueous Tris-buffer (pH = 7). The absorption coefficient spectrum of this cell suspension is shown in Fig. 2a. The absorption peak around 750 nm belongs to the Q_y-band of Bchlc in the chlorosomes, and the absorption peak around 455 nm is due to the Soret band of Bchlc in the chlorosomes. The absorption shoulder around 510 nm comes from the absorption of carotenoids (mainly chlorobactene [25–27]). The tail around 820 nm is due to bacteriochlorophyll a (Bchla) absorption.

For the photo-degradation studies of Bchlc molecules, the cells and the chlorosomes were destroyed by mixing one part of the stock cell culture with nine parts of an acetone/methanol mixture of 7:2 volume parts giving a solution which consists of 70 vol.% acetone, 20 vol.% methanol, and 10 vol.% water. The resulting suspension was filtered to get rid of non-dissolved compartments. Besides Bchlc the cells contain carotenoids (12.1 mol% compared to Bchlc, mainly chlorobactene [25–27]), quinones (14.5 mol%), quinone-like products (40 mol%) [26], and Bchla (2.9 mol%) [25,26] which are partly extracted. The absorption coefficient spectrum of the solution is shown in Fig. 2b. The contribution of Bchla to the absorption spectrum is shown by the dashed curve (taken from [28], absorption cross-section σ (770 nm) $= 2.6 \times 10^{-16}$ cm^2, molar decadic extinction coefficient ε_m (770 nm) $= 6.8 \times 10^4$ dm^3 mol^{-1} cm^{-1} [29], the conversion between σ and ε_m is: $\sigma = \ln(10)\varepsilon_m 1000/N_A$, where N_A is the Avogadro constant). The dash-dotted curve shows the absorption contribution of the carotenoids (taken from [30], σ (490 nm) $= 5.39 \times 10^{-16}$ cm^2, ε_m (490 nm) $= 1.41 \times 10^5$ dm^3 mol^{-1} cm^{-1} [31,32]). The dotted curve shows the absorption contribution of Bchlc (total spectrum minus contribution of Bchla and carotenoids, σ (669 nm) $= 2.68 \times 10^{-16}$ cm^2, ε_m (669 nm) $= 7.0 \times 10^4$ dm^3 mol^{-1} cm^{-1} [33]). In Fig. 2c the bacteriochlorophyll c absorption cross-section spectrum (solid curve) and the bacteriopheophytine c absorption cross-section spectrum (dashed curve) in acetone are displayed (BPhe c spectrum redrawn from [34], σ (669 nm) $\approx 1.55 \times 10^{-16}$ cm^2, ε_m (669 nm) $\approx 4.1 \times 10^4$ dm^3 mol^{-1} cm^{-1} [34]).

Most of the photo-degradation experiments have been carried out by irradiating a sample cell with a cw diode laser operating at 672 nm (power 0.9 mW). For excitation wavelength dependent degradation studies of Bchlc a HeNe laser (wavelength $\lambda_L = 632.8$ mm, power $P = 5$ mW) and a high-pressure mercury lamp ($P = 200$ W) with an interference filter transmitting at $\lambda_L = 428$ nm were used. Depending on the photo-stability the sample cell area was varied and the excitation light optics together with the detection light optics was selected accordingly. A large-area Si photodiode (diameter of sensitive area 1 cm) together with a digital voltmeter and a data storage system are used for light detection. The photodiode was calibrated for absolute power measurement with a power meter (Ophir type PD2-A).

The absorption spectra were measured after fixed periods of light exposure or fixed periods of storage in the dark with a conventional spectrophotometer (Beckman type ACTA M IV). Some absorption spectra of de-aerated samples were measured with a self-assembled spectrometer—diode-array detection system. Comparison of the degraded spectra with known spectra of Bchlc, Bchla, BPhec, and carotenoids will be used to characterize the photoproducts.

3. Experimental results

The photo-degradation of Bchlc in intact *Chlorobium tepidum* cell suspensions and of Bchlc in acetone–methanol–water extracts are investigated. Transmission changes at the excitation wavelength as a function of exposure time and absorption coefficient spectra at some time positions are presented. The temporal degradation of samples in the dark after light exposure is analyzed.

3.1. Photo-stability of intact Chlorobium tepidum cell suspensions

In the dark at room temperature no absorption spectroscopic change was observed within a few days indicating high thermal stability of the chlorosomes in the cells.

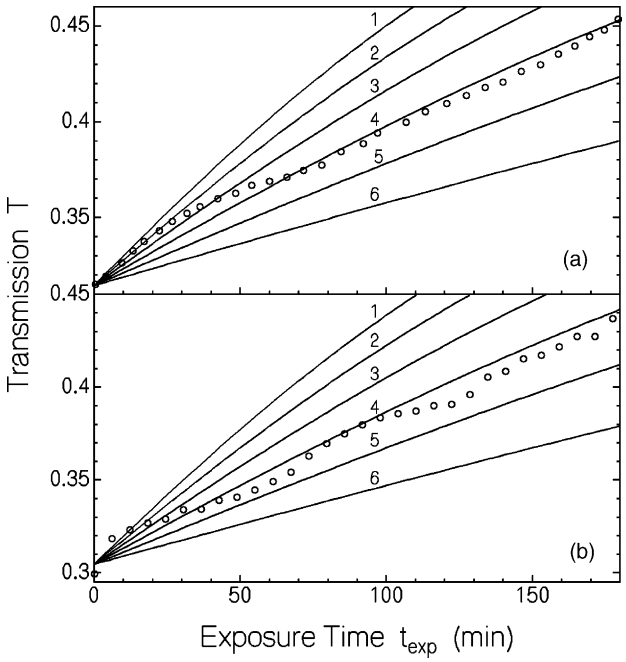

Fig. 3. Dependence of excitation light transmission, T, through *Chlorobium tepidum* cell suspension on exposure time, t_{exp}. Excitation wavelength, $\lambda_L = 784\,nm$. Excitation intensity, $I_L = 0.353\,W\,cm^{-2}$. Cell length $\ell = 2\,cm$. Concentration of Bchlc is $C_{C,0} = 8.8 \times 10^{-6}\,mol\,dm^{-3}$. Scattering contribution is removed from transmission. Solid curves are calculated by use of Eqs. (27) and (28) with effective quantum yields of photo-degradation of $\phi_D = 1.4 \times 10^{-6}$ (1); 1.2×10^{-6} (2); 1.0×10^{-6} (3); 8×10^{-7} (4); 6×10^{-7} (5); and 4×10^{-7} (6): (a) anaerobic suspension; (b) aerobic suspension.

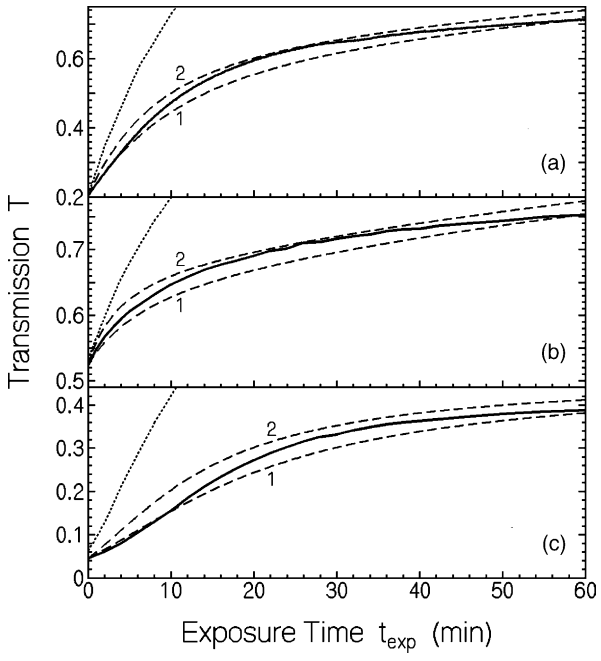

Fig. 4. Time dependent excitation light transmission through air-saturated *Chlorobium tepidum* extract for several excitation wavelengths, λ_L. Cell length $\ell = 2\,cm$. Thick solid curves are measured, dotted curves give contribution of Bchlc to transmission, and dashed curves are calculated (Eqs. (20)–(22)). (a) $\lambda_L = 672\,nm$, $I_L = 0.8\,mW\,cm^{-2}$, and $N_{C,0} = C_{C,0}N_A = 4.2 \times 10^{15}\,cm^{-3}$, $j = CI$. Curve 1, $\phi_{D,0} = 0.009$, $\sigma_{L,CI}\beta_{CI} = 4.2 \times 10^{-17}\,cm^2$, $\kappa_{CIP}N_{^3O_2} = 1.32 \times 10^{-4}\,s^{-1}$, $\alpha_{L,res} = 0$. Curve 2, $\phi_{D,0} = 0.013$, $\sigma_{L,CI}\beta_{CI} = 4.2 \times 10^{-17}\,cm^2$, $\kappa_{CIP}N_{^3O_2} = 1.32 \times 10^{-4}\,s^{-1}$, $\alpha_{L,res} = 0$. (b) $\lambda_L = 632.8\,nm$, $I_L = 1.21\,mW\,cm^{-2}$, and $N_{C,0} = 4.9 \times 10^{15}\,cm^{-3}$, $J = D$. Curve 1, $\phi_{D,0} = 0.012$, $\sigma_{L,D}\beta_D = 3.6 \times 10^{-17}\,cm^2$, $\kappa_{DP}N_{^3O_2} = 1.32 \times 10^{-4}\,s^{-1}$, $\alpha_{L,res} = 0$. Curve 2, $\phi_{D,0} = 0.024$, $\sigma_{L,D}\beta_D = 3.6 \times 10^{-17}\,cm^2$, $\kappa_{DP}N_{^3O_2} = 1.32 \times 10^{-4}\,s^{-1}$, $\alpha_{L,res} = 0$. (c) $\lambda_L = 428\,nm$, $I_L = 0.47\,mW\,cm^{-2}$, and $N_{C,0} = 4.65 \times 10^{15}\,cm^{-3}$, $J = D$. Curve 1, $\phi_{D,0} = 0.016$, $\sigma_{L,D}\beta_D = 5.5 \times 10^{-17}\,cm^2$, $\kappa_{DP}N_{^3O_2} = 0\,s^{-1}$, $\alpha_{L,res} = 0.142\,cm^{-1}$. Curve 2, $\phi_{D,0} = 0.024$, $\sigma_{L,D}\beta_D = 5.5 \times 10^{-17}\,cm^2$, $\kappa_{DP}N_{^3O_2} = 0\,s^{-1}$, $\alpha_{L,res} = 0.142\,cm^{-1}$.

Light irradiation at room temperature causes a gradual rise in transmission both under aerobic and anaerobic conditions (nitrogen bubbling through sample for several hours). The rises in transmission versus exposure time for an anaerobic sample and for the aerobic sample are shown in Fig. 4a and b, respectively. The light exposure parameters are given in the figure caption. A numerical simulation of the absorption and degradation dynamics (see Eqs. (27) and (28), and solid curves in Fig. 3) indicates a very low quantum yield of photo-degradation.

3.2. Photo-stability of bacteriochlorophyll c in acetone–methanol–water extract from Chlorobium tepidum

For the air-saturated extracts from *Chlorobium tepidum* containing Bchlc, Bchla, carotenoids and quinones no transmission changes were observed in the dark at room temperature within a few days. Even at an elevated temperature of 60 °C no spectral changes were observed after 24 h. These findings indicate a high thermal stability of these compounds in the absence of light.

The transmission changes of air-saturated extracts from *Chlorobium tepidum* in acetone–methanol–water solution for three different excitation wavelengths, λ_L, are shown by thick solid curves in Fig. 4. In Fig. 4a the excitation wavelength is $\lambda_L = 672\,nm$ (excitation on long-wavelength side of Q_y-band of Bchlc). Initially the transmission rises steeply (Bchlc degradation), and at long exposure times the rise in transmission slows down (photoproduct formation which absorbs at 672 nm and has a higher photo-stability). In Fig. 4b the excitation wavelength is $\lambda_L = 632.8\,nm$ (short-wavelength side of Q_y-band of Bchlc). Again a steep initial rise in transmission and a slowing down in transmission rise are observed. In Fig. 4c the excitation wavelength is 428 nm (short-wavelength side of Soret band). The transmission behavior is similar to excitation into the Q_y-band (Fig. 4a and b).

Spectral changes of the absorption coefficient spectra after certain times of sample irradiation at $\lambda_L = 672\,nm$ are displayed in Fig. 5a. A logarithmic ordinate scale is used to get a better separation of the curves. The initial absorption contribution of the carotenoids is subtracted for better observation of the Bchlc degradation. There is no indication of carotenoid degradation. The Q_y-band

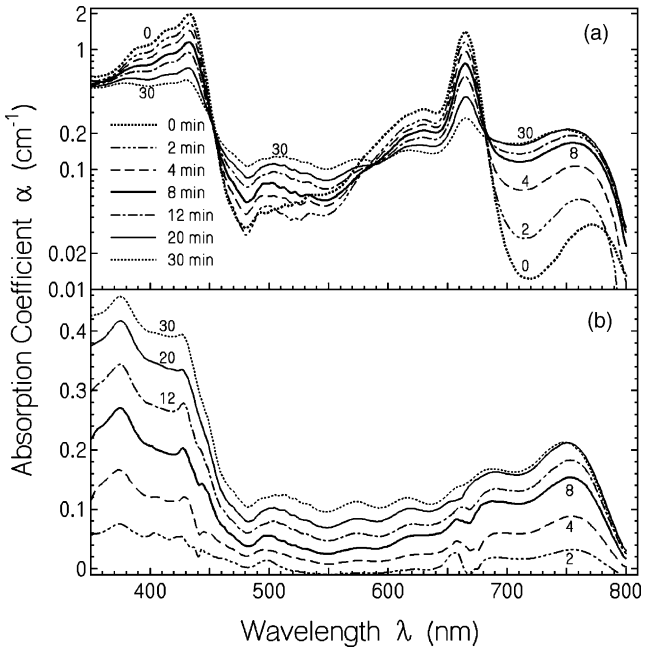

Fig. 5. (a) Absorption coefficient spectra, $\alpha(\lambda)$, of air-saturated *Chlorobium tepidum* extract after different times of exposure. $\lambda_L = 672$ nm and $I_L = 0.41\,mW\,cm^{-2}$. Carotene contribution is subtracted. (b) Absorption coefficient spectra of part (a) after approximate subtraction of Bchlc contribution which is not yet degraded.

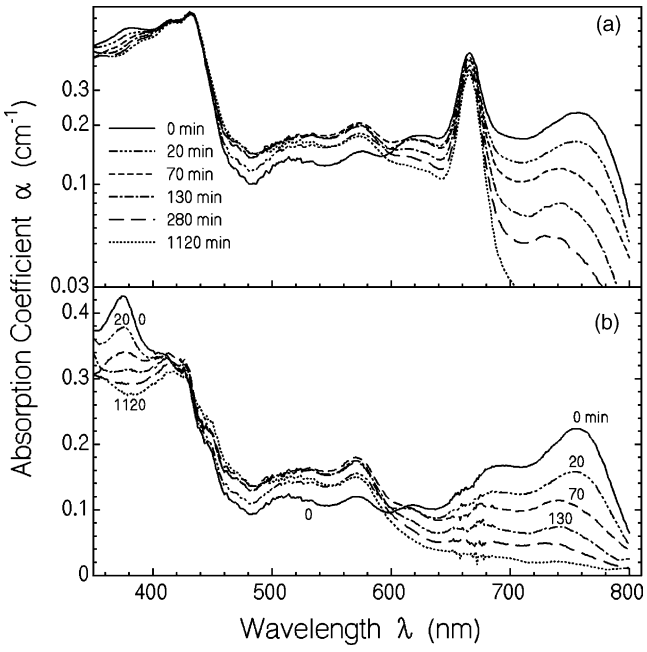

Fig. 6. (a) Absorption coefficient spectra of air-saturated *Chlorobium tepidum* extract in the dark for several times after 10 min laser light exposure at $\lambda_L = 672$ nm with $I_L = 0.74\,mW\,cm^{-2}$. Storage times are given in the legend. Carotene contribution is subtracted. (b) Absorption coefficient spectra of part (a) after subtraction of Bchlc contribution.

absorption (peak around 665 nm) and the Soret-band absorption (peak around 435 nm) reduce due to Bchlc degradation. A new absorption band is built up around 750 nm which will be attributed to the formation of bacteriochlorophyll a-like molecules (Bchla-I and Bchla-II, structure in Fig. 1c). Additionally some increase in absorption occurs in the wavelength range from 590 to 460 nm due to Bchlc-peroxide formation with subsequent ring cleavage to linear tetrapyrrole structures (8-acetylbiltriene structures [35], also called photobiline-like structures [35], see Fig. 1d and e) [13,17–24]. The slowed-down absorption decrease in the 350–400 nm range is thought to be due to Bchla-I and Bchla-II formation. The spectra deprived of BChl c absorption (subtraction without discontinuous curve formation) are shown in Fig. 5b on a linear ordinate scale. They clearly reveal the build-up of an absorption band around 690 nm (isobestic point in Fig. 5a). This band is thought to be due to some changes of Bchlc (probably oxidation of the hydroxyl group at the C3 position to a keto group). This photoproduct we called Bchlc-I. Comparing the spectra in Fig. 5b with the bacteriopheophytine c (Bphec) spectrum of Fig. 2c there is no indication of Bphec formation in the photo-degradation process (Q_x-band in the 500–560 nm region does not show up).

For sample irradiation at $\lambda_L = 632.8$ and 428 nm similar spectral dependencies have been observed as for $\lambda_L = 672$ nm (the curves are not shown).

Photo-excitation at 470 nm (excitation intensity $0.53\,mW\,cm^{-2}$, exposure time 30 min), where Bchlc is only weakly absorbing and the carotenoids are strongly absorbing (see Fig. 2b), showed up in no measurable transmission changes of the carotenoids (curve not shown here). This indicates that the present carotenoids have a high photo-stability.

The temporal degradation of an air-saturated extract after light exposure is studied in Fig. 6. The sample was irradiated for 10 min at $\lambda_L = 672$ nm with laser light of $0.74\,mW\,cm^{-2}$ intensity. Measured absorption coefficient spectra deprived from the carotenoid contribution at several times after the light exposure are shown in Fig. 6a (logarithmic ordinate). The absorption spectra approximately deprived from the Bchlc contribution are displayed in Fig. 6b (linear ordinate). The long-wavelength absorption above 600 nm decreases with time. The formed broad absorption band around 750 nm is thought to consist of two main bands one centered at 760 nm (Bchla-I) and the other centered at 730 nm (Bchla-II). The 760 nm band degrades slightly faster than the 730 nm band. Therefore the absorption peak shifts from 760 to 730 nm with time. The absorption band around 690 nm (Bchlc-I) decreases with a similar speed as the Bchla-II band. The degradation is thought to be caused by oxidizing species (most likely triplet oxygen $^3O_2$). The Bchlc band remains unchanged (no temporal degradation in the dark). In the wavelength range from 440 to 600 nm a slight increase in absorption is observed due to degradation of Bchla-I, Bchla-II, and Bchlc-I to linear tetrapyrroles. The linear tetrapyrroles seem to be stable. The absorption reduction in the 350–400 nm range is thought to be due to degradation of Bchla-I, and Bchla-II molecules which absorb in this wavelength region.

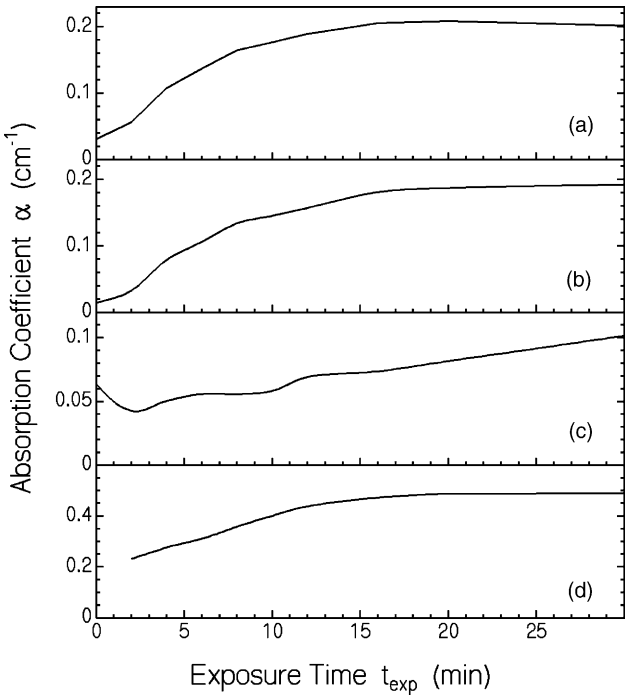

Fig. 7. Absorption coefficients, α, of air-saturated *Chlorobium tepidum* extract deprived from carotenoid contributions vs. exposure time, t_{exp}, at selected wavelengths. Excitation wavelength $\lambda_L = 672$ nm and excitation intensity $I_L = 0.41\,mW\,cm^{-2}$. The detection wavelengths are: (a) $\lambda_{pr} = 760$ nm; (b) $\lambda_{pr} = 730$ nm; (c) $\lambda_{pr} = 550$ nm; and (d) $\lambda_{pr} = 375$ nm.

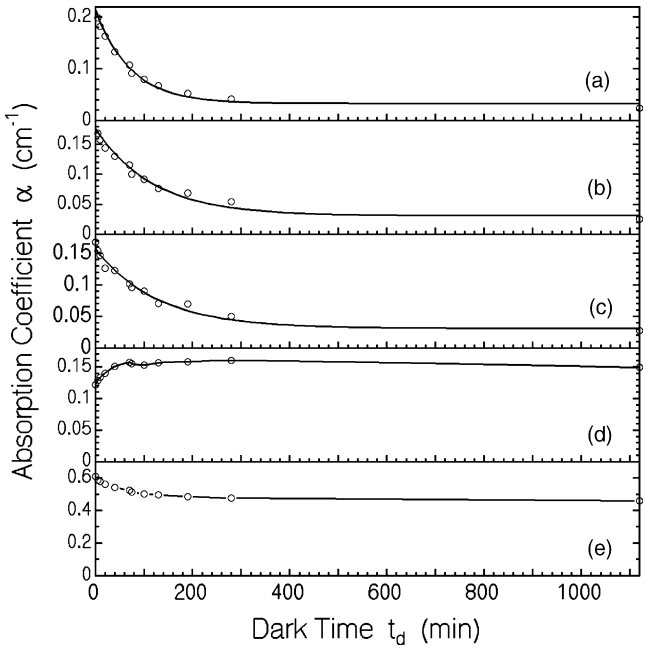

Fig. 8. Absorption coefficients, α, of air-saturated *Chlorobium tepidum* extract in the dark deprived from carotenoid contribution vs. dark time, t_d, after light exposure ($\lambda_L = 672$ nm, $t_{exp} = 10$ min, $I_L = 0.74\,mW\,cm^{-2}$) at selected detection wavelengths λ_{pr}. Circles are measured. Curves in (a–c) are fits using $\alpha(t_d) = \alpha_0 \exp(-t_d/\tau) + \alpha_{res}$. (a) $\lambda_{pr} = 760$ nm (dominant Bchla-I). $\alpha_0 = 0.16\,cm^{-1}$, $\alpha_{res} = 0.0589$, $\tau = 51$ min; (b) $\lambda_{pr} = 730$ nm (dominant Bchl-II). $\alpha_0 = 0.145\,cm^{-1}$, $\alpha_{res} = 0.031\,cm^{-1}$, $\tau = 118.4$ min. (c) $\lambda_{pr} = 690$ nm (dominant Bchlc-I). $\alpha_0 = 0.126\,cm^{-1}$, $\alpha_{res} = 0.031\,cm^{-1}$, $\tau = 126.4$ min. (d) $\lambda_{pr} = 500$ nm (dominant linear tetrapyrrole). (e) $\lambda = 375$ nm (Bchlc, Bchlc-I, Bchla-I, Bchla-II).

The changes of the extract absorption coefficients deprived from carotenoid contributions at selected wavelengths versus exposure time are illustrated in Fig. 7 for excitation at 672 nm (Fig. 5). A re-plotting of Fig. 5a at fixed detection wavelengths is done. Fig. 7a shows the absorption build-up and decrease at 760 nm (expected absorption maximum of Bchla-I). Fig. 7b shows the build-up (at longer exposure times a decrease occurs) of absorption at 730 nm (expected absorption maximum of Bchla-II). Fig. 7c depicts the rise of absorption at 550 nm (expected linear tetrapyrrole formation). Fig. 7d shows the absorption rise and leveling-off at 375 nm (at longer exposure times a slight decrease occurs). This behavior is similar to the absorption rise and decrease at 760 and 730 nm (changes are expected to be due to Bchla-I and Bchla-II build-up and subsequent degradation).

The temporal absorption changes after light exposure are illustrated in Fig. 8 (re-plotting of data at 760, 730, 500 and 375 nm from Fig. 6a, and at 690 nm from Fig. 6b). At $\lambda_{pr} = 760$, 730, and 690 nm the absorption decrease is fitted reasonably well by a single exponential decay and a constant pedestal. The decay times are τ(Bchla-I) = 51 min, τ(Bchla-II) = 118.4 min, and τ(Bchlc-I) = 126.4 min. The rise in absorption at 500 nm (Fig. 8d) is thought to be due linear tetrapyrrole formation by degradation of the longer-wavelength absorbing components (Bchla-I, Bchla-II, Bchlc-I). The decrease in absorption at 375 nm (Fig. 8e) is attributed to the degradation of Bchla-I, Bchla-II, and Bchlc-I.

De-oxygenation of the extract by nitrogen bubbling reduces the quantum yield of photo-degradation. In Fig. 9 the temporal change of transmission is shown in the case of excitation at 672 nm (thick solid curve). Some absorption spectra after certain times of exposure are depicted in Fig. 10. The spectral shapes are somewhat different from the spectral shapes of the aerated samples. This difference is illustrated in Fig. 10b where a curve from Fig. 5b (air-saturated sample exposed at 672 nm for 30 min) is overlaid. It indicates that for the nitrogen-bubbled sample the intermediate photoproducts are somewhat different from those of the air-saturated samples.

The dark degradation of a de-oxygenated sample which was exposed to light at 672 nm for 150 min is shown in Fig. 11. The Bchlc content remains unchanged in the dark (no thermal degradation). The photoproducts which absorb at wavelengths longer than 530 nm degrade slowly in the dark. In the wavelength region below 530 nm the absorption increases with time due to the degradation of the longer-wavelength photoproducts to stable short-wavelength photoproducts.

The long-wavelength photoproducts degrade approximately exponential in the dark as is shown in Fig. 12 (data points taken form Fig. 11b). The thermal dark decay of the intermediate photoproducts is approximately a factor of 15

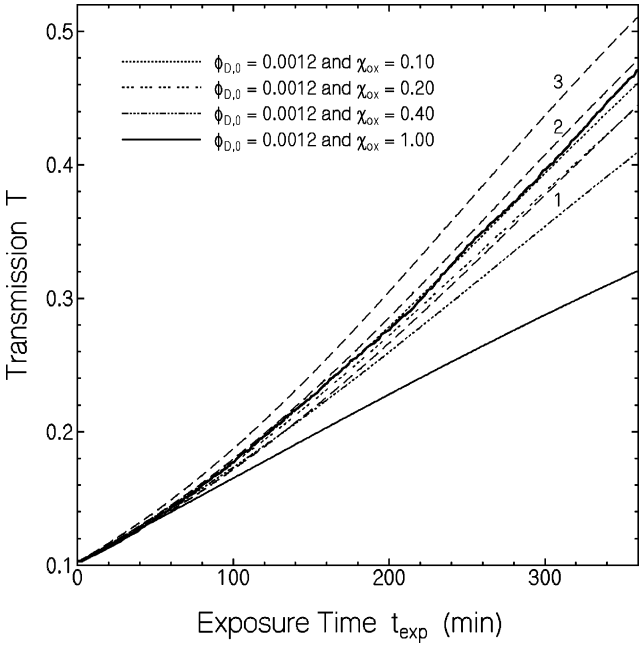

Fig. 9. Excitation light transmission vs. exposure time through N_2-bubbled *Chlorobium tepidum* extract (bubbling for 6 h). $\lambda_L = 672$ nm, $I_L = 0.17\,mW\,cm^{-2}$, $\ell = 1.5$ cm, $N_{C,0} = 8.0 \times 10^{15}\,cm^{-3}$. Thick solid curve is measured. Dashed curves are calculated using Eqs. (20)–(22) with $\sigma_{L,CI}\beta_{CI} = 2.81 \times 10^{-17}\,cm^2$, $\alpha_{L,res} = 0$, $k_{CIP} = 9.3 \times 10^{-6}\,s^{-1}$. Curve 1, $\phi_{D,0} = 0.0011$ and $\chi_T = 1$; curve 2, $\phi_{D,0} = 0.0012$ and $\chi_T = 1$; curve 3, $\phi_{D,0} = 0.0013$ and $\chi_T = 1$. Other curves are explained in legend.

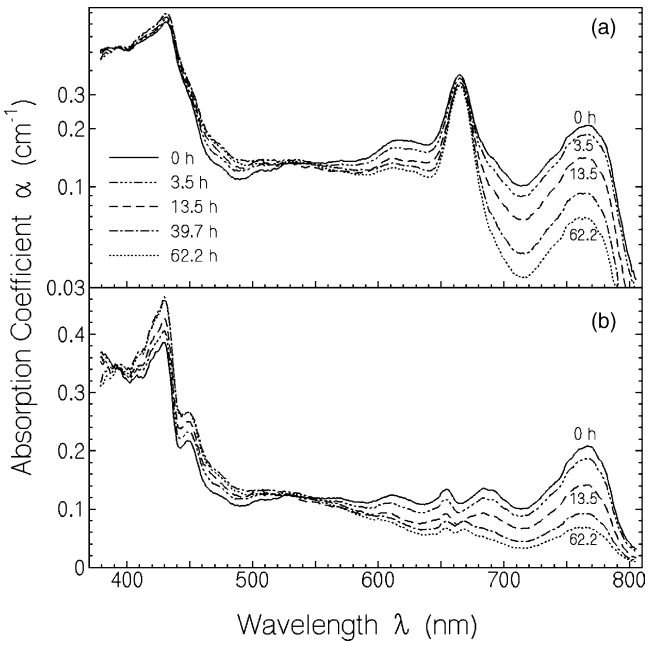

Fig. 11. (a) Absorption coefficient spectra of nitrogen-bubbled *Chlorobium tepidum* extract in the dark for several times after 150 min of laser light exposure at $\lambda_L = 672$ nm with $I_L = 0.19\,mW\,cm^{-2}$. Storage times are given in the legend. Carotene contribution is subtracted. (b) Absorption coefficient spectra of part (a) after subtraction of remaining Bchlc contribution.

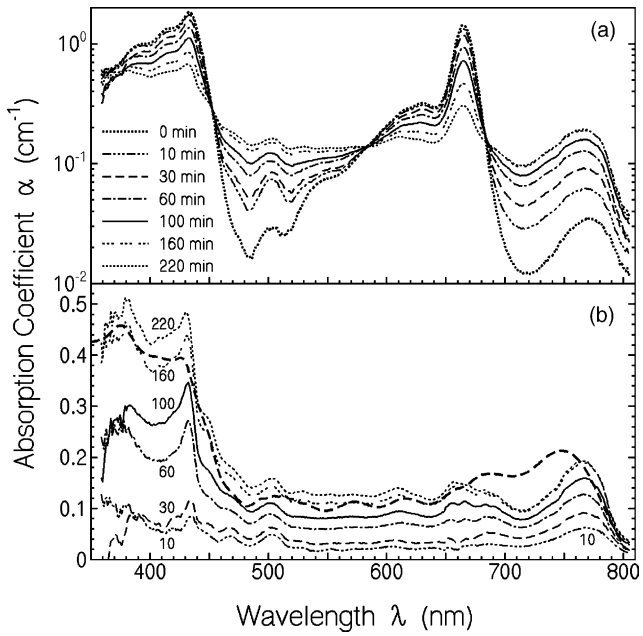

Fig. 10. (a) Absorption coefficient spectra of N_2-bubbled *Chlorobium tepidum* extract after different times of exposure (bubbling for 6 h). $\lambda_L = 672$ nm and $I_L = 0.19\,mW\,cm^{-2}$. Cell length, $\ell = 1.5$ cm. Carotene contribution is subtracted. Exposure times are listed in figure. (b) Absorption coefficient spectra of part (a) after approximate subtraction of remaining Bchlc contribution. Thick dashed curve is taken from Fig. 5b ($t_{exp} = 30$ min) for comparison.

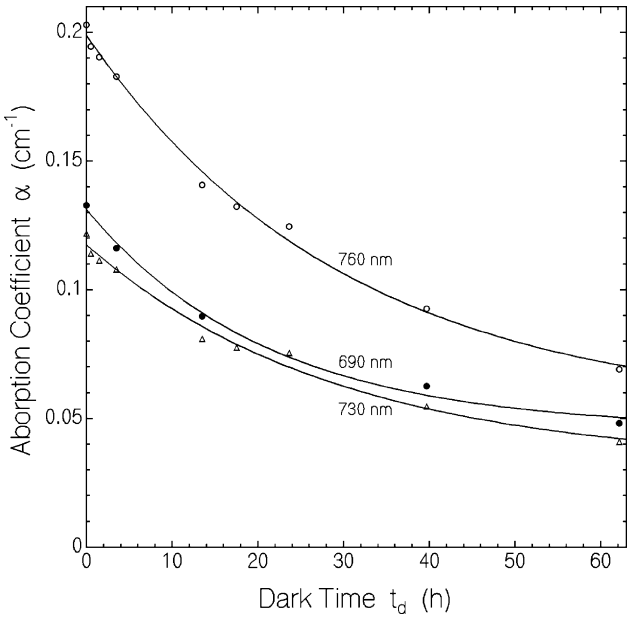

Fig. 12. Absorption coefficients, α, of N_2-bubbled *Chlorobium tepidum* extract in the dark deprived from carotenoid contribution vs. dark time, t_d, after light exposure ($\lambda_L = 672$ nm, $t_{exp} = 150$ min, $I_L = 0.19\,mW\,cm^{-2}$) at selected detection wavelengths λ_{pr}. Circles are measured. Curves are fits by $\alpha(t_d) = \alpha_0 \exp(-t_d/\tau) + \alpha_{res}$. For $\lambda_{pr} = 760$ nm: $\alpha_0 = 0.147\,cm^{-1}$, $\alpha_{res} = 0.052$, $\tau = 30.1$ h. For $\lambda_{pr} = 730$ nm: $\alpha_0 = 0.0853\,cm^{-1}$, $\alpha_{res} = 0.032\,cm^{-1}$, $\tau = 29.1$ h. For $\lambda_{pr} = 690$ nm: $\alpha_0 = 0.0851\,cm^{-1}$, $\alpha_{res} = 0.046\,cm^{-1}$, $\tau = 21.2$ h.

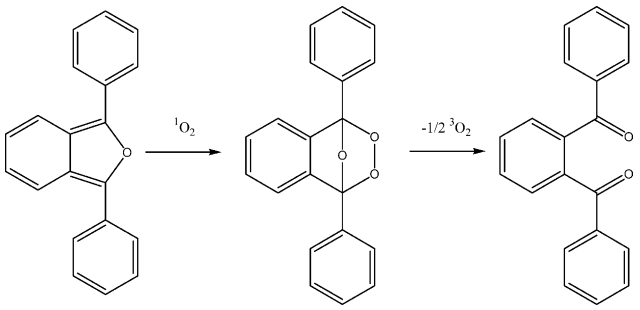

Scheme 1. Singlet-oxygen consumption by DPBF.

slowed down in the de-oxygenated samples compared to the air-saturated samples.

The triplet oxygen content of the N_2-bubbled sampled was determined by adding the singlet-oxygen scavenger 1,3-diphenylisobenzofuran (DPBF) [36] to the nitrogen-bubbled solution. This compound is very reactive with singlet oxygen by peroxide formation (DPBF-O_2) and subsequent reaction to o-dibenzoylbenzene (DBB) according to the reaction Scheme 1.

Photo-excitation of Bchlc generates triplet Bchlc, the triplet Bchlc reacts with triplet oxygen to generate singlet oxygen which is consumed by DPBF. The process continues until all $^3O_2$ is consumed. DPBF has an absorption peak at 410 nm while DBB is transparent there. The transmission increase allows the evaluation of the oxygen content. Our analysis gives a value of $C_{3_{O_2}} \approx 1 \times 10^{-5}\,\mathrm{mol\,dm^{-3}}$ for the N_2-bubbled samples (6 h of bubbling). Bubbling with Argon practically gave the same result.

4. Theoretical analysis

The photo-degradation dynamics of Bchlc in the chlorosomes of intact *Chlorobium tepidum* cell suspensions, and of Bchlc from *Chlorobium tepidum* extracts in air-saturated and de-aerated acetone–methanol–water solutions is studied in the following. A detailed equation system is developed for the Bchlc solutions including degradation directly from photo-excited states and oxidative degradation from self-generated singlet oxygen. For the highly photo-stable Bchlc in the chlorosomes of intact *Chlorobium tepidum* cells a simple degradation scheme is used to determine the quantum yield of photo-degradation.

4.1. Photo-stability of bacteriochlorophyll c in solution

In air-containing acetone–methanol–water solution Bchlc produces singlet oxygen after photo-excitation in the singlet system and subsequent intersystem-crossing to the triplet system. The singlet oxygen causes degradation of Bchlc (quantum yield of oxidative degradation, $\phi_{D,ox}$) by (i) Bchlc per-oxidation and subsequent ring cleavage to linear tetrapyrroles at the C1–C20 position or C19–C20 position [13,17–24] (see Fig. 1); (ii) Bchlc oxidation at the C7–C8 position to structures with Bchla-like absorption (double bond removal, Bchla-I and Bchla-II formation with different absorption peaks); and (iii) modification of Bchlc to a derivative (called Bchlc-I) with an absorption peak around 690 nm (likely oxidation of hydroxy-ethyl group at C3 position to keto-ethyl group). The photo-oxidized bacteriochlorophylls, Bchla-I, Bchla-II, Bchlc-I, degrade in the dark at room temperature. The dissolved oxygen (ground-state triplet-oxygen, $^3O_2$) catalyzes the degradation.

Even without any oxygen present, direct excited-state degradation of Bchlc in solution occurs after photo-excitation as will come out from the data analysis. The degradation from singlet excited molecules (quantum yield of degradation of singlet excited molecules, ϕ_{SD}) is thought to be negligibly small compared to the degradation from triplet excited molecules (quantum yield of degradation of triplet excited molecules, ϕ_{TD}) because of the much longer triplet-state lifetime compared to the singlet-state lifetime. The direct degradation of triplet Bchlc produces slightly different absorbing species, Bchla-I′, Bchla-II′, Bchlc-I′, than the oxidative degradation. This slight difference is neglected in the following equation system, i.e. the number densities of Bchla-I and Bchla-I′ are comprised to $N_{AI_g} = N_{AI} + N_{AI'}$, and similar we use $N_{AII_g} = N_{AII} + N_{AII'}$, as well $N_{CI_g} = N_{CI} + N_{CI'}$.

The carotenoids present in the Bchlc solutions indirectly influence the quantum yield of photo-degradation by reducing the triplet-state lifetime.

The excitation and degradation processes for Bchlc in oxygen-containing solution are listed in the following Scheme 2.

The excitation light at wavelength λ_L (frequency ν_L) excites Bchlc in the singlet ground-state (^{1}Bchlc, number density N_{S0}) to a singlet excited-state (^{1}Bchl*, N_{S1}). From there part of the molecules (quantum yield ϕ_T) relaxes to the triplet state (^{3}Bchlc*, N_T), others return to the singlet ground-state (rate k_{10}), and a small amount may degrade (quantum yield ϕ_{SD}). The molecules in the triplet state return partly to the singlet ground-state by intersystem-crossing (rate k_{TS}), partly they return to the ground-state by reaction with triplet oxygen whereby singlet oxygen is formed (bimolecular rate κ_{TO}), and a part of them degrades to linear tetrapyrrole (LTP, rate k_{TD}), Bchla-I′ (rate k_{TAI}), Bchla-II′ (rate k_{TAII}), and Bchlc-I′ (rate k_{TCI}). The generated singlet oxygen (number density $N_{1_{O_2}}$) relaxes to ground-state triplet oxygen, $^3O_2$, with a time constant k_{O13}. On the other hand, $^1O_2$ reacts within its lifetime, $\tau_{1_{O_2}}$ ($\approx k_{O13}^{-1}$), with ground-state Bchlc to a per-oxide (Bchlc-O_2, bimolecular rate κ_{OP}) which is expected to disintegrate immediately to linear oxidized tetrapyrroles (LTP), it forms Bchla-I (reaction constant κ_{OAI}), Bchla-II (reaction constant κ_{OAII}), and Bchlc-I (reaction constant κ_{OCI}). The generated photoproducts degrade in the dark to linear tetrapyroles with rate constants k_{AIP} for Bchla-I′ and Bchla-I, k_{AIIP} for Bchla-II′ and Bchla-II, and k_{CIP} for

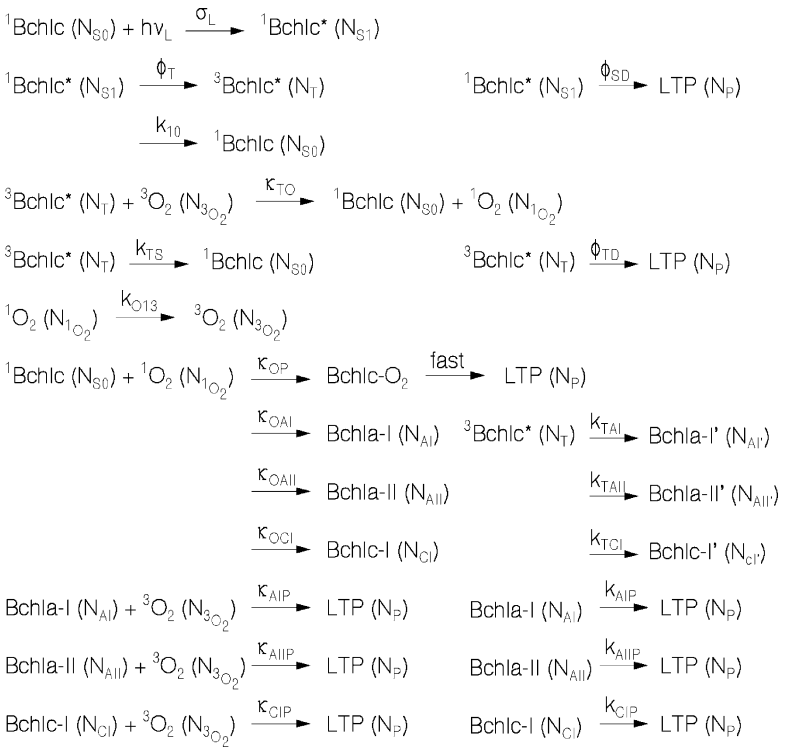

Scheme 2. Photo-degradation dynamics of Bchlc.

Bchlc-I′ and Bchlc-I, and they degrade in bi-molecular reaction with $^3O_2$ with the reaction constants κ_{AIP} (Bchla-I), κ_{AIIP} (Bchla-II), and κ_{CIP} (Bchlc-I). The excitation light at frequency ν_L and the probe light of frequency ν_{pr} are absorbed with the absorption cross-sections $\sigma_{L,i}$ and $\sigma_{pr,i}$ of the present compounds i at the relevant wavelengths. Some residual absorption with coefficients $\alpha_{L,res}$ and $\alpha_{pr,res}$ from weakly interacting or non-interacting molecules (like carotenoids) may be present.

The degradation of the small amount of Bchla present in the extract is neglected here. It is studied separately in [37].

The excitation and relaxation dynamics presented in Scheme 2 may be described by the following rate equation system for the number densities, N_i, and the excitation light intensity, I_L [38]:

$$\frac{\partial N_{S0}}{\partial t} = -\frac{\sigma_L}{h\nu_L} I_L N_{S0} + (1-\phi_T-\phi_{SD})\frac{N_{S1}}{\tau_F} + (k_{TS}+\kappa_{TO}N_{^3O_2})N_T - (\kappa_{OP}+\kappa_{OAI}+\kappa_{OAII}+\kappa_{OCI})N_{^1O_2}N_{S0}, \quad (1)$$

$$\frac{\partial N_{S1}}{\partial t} = \frac{\sigma_L}{h\nu_L} I_L N_{S0} - \frac{N_{S1}}{\tau_F}, \quad (2)$$

$$\frac{\partial N_T}{\partial t} = \phi_T \frac{N_{S1}}{\tau_F} - (k_{TS}+k_{TD}+\kappa_{TO}N_{^3O_2})N_T, \quad (3)$$

$$\frac{\partial N_{^1O_2}}{\partial t} = \kappa_{TO}N_{^3O_2}N_T - k_{O13}N_{^1O_2} - \kappa_{ox}N_{S0}N_{^1O_2}, \quad (4)$$

$$\frac{\partial N_{AI_g}}{\partial t} = k_{TAI}N_T + \kappa_{OAI}N_{S0}N_{^1O_2} - (k_{AIP}+\kappa_{AIP}N_{^3O_2})N_{AI_g}, \quad (5)$$

$$\frac{\partial N_{AII_g}}{\partial t} = k_{TAII}N_T + \kappa_{OAII}N_{S0}N_{^1O_2} - (k_{AIIP}+\kappa_{AIIP}N_{^3O_2})N_{AII_g}, \quad (6)$$

$$\frac{\partial N_{CI_g}}{\partial t} = k_{TCI}N_T + \kappa_{OCI}N_{S0}N_{^1O_2} - (k_{CIP}+\kappa_{CIP}N_{^3O_2})N_{CI_g}, \quad (7)$$

$$\frac{\partial N_P}{\partial t} = \kappa_{OP}N_{S0}N_{^1O_2} + (\kappa_{AIP}N_{AI_g}+\kappa_{AIIP}N_{AII_g} + \kappa_{CIP}N_{CI_g})N_{^3O_2} + k_{AIP}N_{AI_g} + k_{AIIP}N_{AII_g} + k_{CIP}N_{CI_g} + \phi_{SD}\frac{N_{S1}}{\tau_F} + k_{TP}N_T, \quad (8)$$

$$\frac{\partial I_L}{\partial z} = -(\sigma_L N_{S0} + \sigma_{L,CI}N_{CI_g} + \sigma_{L,AI}N_{AI_g} + \sigma_{L,AII}N_{AII_g})I_L - \alpha_{L,res}I_L. \quad (9)$$

The abbreviations $\kappa_{ox} = \kappa_{OP}+\kappa_{OAI}+\kappa_{OAII}+\kappa_{OCI}$ and $k_{TD} = k_{TAI}+k_{TAII}+k_{TCI}$ are used.

The initial conditions are

$$I_L(t=0,z) = \begin{cases} I_L & \text{for } t \geq 0 \\ 0 & \text{for } t < 0 \end{cases}, \quad (10)$$

$$N_{S0}(t=0,z) = N_{C,0}, \quad (11a)$$

$$N_j(t=0,z)=0, \quad \text{for } j=\mathrm{S1, T, AI_g, AII_g, CI_g, P.} \tag{11b}$$

The transmission behaviour of a weak probe light of intensity I_{pr} at wavelength λ_{pr} is governed by

$$\frac{\partial I_{pr}}{\partial z} = -(\sigma_{pr}N_{S0} + \sigma_{pr,AI}N_{AI_g} + \sigma_{pr,AII}N_{AII_g} + \sigma_{pr,CI}N_{CI_g})I_{pr} - \alpha_{pr,res}I_{pr}, \tag{12}$$

The light transmission is calculated by $T_i = I_i(z=\ell)/I_i(z=0)$, $i = \mathrm{L, pr}$, where z is the propagation coordinate, and ℓ is the sample length.

Steady-state conditions are reached for intermediates at times longer than a few times the relevant relaxation times. Under steady-state conditions the time derivates may be set to zero, i.e. $\partial/\partial t = 0$. These intermediates are ^{1}Bchlc* (N_{S1}, lifetime τ_F in ns region [39], own measurement gives $\tau_F = 24.5 \pm 1$ ns), ^{3}Bchlc* (N_T, lifetime τ_T in μs region [22–24], value of $\tau_T = 250 \pm 40$ ns for Bchlc in air-saturated acetone is given in [22]), and $^1O_2$ ($N_{^1O_2}$, lifetime $\tau_{^1O_2} = k_{O13}^{-1}$ in μs region [40], explicit values are $\tau_{^1O_2} = 2$ μs in water, $\tau_{^1O_2} = 7$ μs in methanol, and $\tau_{^1O_2} = 26$ μs in acetone [40]). The singlet-oxygen relaxation is governed by the term $N_{^1O_2}/\tau_{^1O_2}$ (return to $^3O_2$ by intersystem crossing and reaction with solvent molecules), therefore the term $\kappa_{ox}N_{^1O_2}N_{S0}$ due to bacteriochlorophyll c oxidation in Eq. (4) is negligible (as long as the quantum yield of Bchlc photo-degradation is small compared to 1). The quenching of singlet oxygen by bacteriochlorophyll c in a charge-transfer deactivation process [41] according to $^1\mathrm{Bchlc} + {}^1O_2 \rightarrow (^1\mathrm{Bchlc}\cdots{}^1O_2) \rightarrow {}^1\mathrm{Bchlc} + {}^3O_2$ is neglected in our diluted solutions [22].

These conditions lead to

$$N_{S1} = \frac{\sigma_L\tau_F}{h\nu_L}I_L N_{S0}, \tag{13a}$$

$$N_T = \frac{\phi_T}{\tau_F(k_{TS}+k_{TD}+\kappa_{TO}N_{^3O_2})}N_{S1} = \phi_T\frac{\sigma_L}{h\nu_L(k_{TS}+k_{TD}+\kappa_{TO}N_{^3O_2})}I_L N_{S0}, \tag{13b}$$

$$N_{^1O_2} = \frac{\kappa_{TO}}{k_{O13}+\kappa_{ox}N_{S0}}N_{^3O_2}N_T = \phi_T\frac{\sigma_L\kappa_{TO}}{h\nu_L(k_{O13}+\kappa_{ox}N_{S0})(k_{TS}+k_{TD}+\kappa_{TO}N_{^3O_2})} \times I_L N_{^3O_2}N_{S0}, \tag{13c}$$

for the short-living intermediates.

Eqs. (1) and (5)–(8) reduce to

$$\frac{\partial N_{S0}}{\partial t} = -(\phi_{SD}+\phi_T\phi_{TD})\frac{\sigma_L}{h\nu_L}I_L N_{S0} - \kappa_{ox}N_{^1O_2}N_{S0} = -\frac{\sigma_L}{h\nu_L}I_L N_{S0}\left\{\phi_{SD}+\phi_T\phi_{TD}+\phi_T\frac{\kappa_{ox}\kappa_{TO}}{(k_{O13}+\kappa_{ox}N_{S0})(k_{TS}+k_{TD}+\kappa_{TO}N_{^3O_2})}N_{^3O_2}N_{S0}\right\} = -\frac{\sigma_L}{h\nu_L}I_L N_{S0}(\phi_{D,S}+\phi_{D,T}+\phi_{D,ox}) = -\frac{\sigma_L}{h\nu_L}I_L N_{S0}\phi_D \tag{14}$$

$$\frac{\partial N_{AI_g}}{\partial t} = \frac{\sigma_L}{h\nu_L}I_L N_{S0}\left(\frac{k_{TAI}}{k_{TD}}\phi_{D,T}+\frac{\kappa_{OAI}}{\kappa_{ox}}\phi_{D,ox}\right) - (k_{AIP}+\kappa_{AIP}N_{^3O_2})N_{AI_g}, \tag{15}$$

$$\frac{\partial N_{AII_g}}{\partial t} = \frac{\sigma_L}{h\nu_L}I_L N_{S0}\left(\frac{k_{TAII}}{k_{TD}}\phi_{D,T}+\frac{\kappa_{OAII}}{\kappa_{ox}}\phi_{D,ox}\right) - (k_{AIIP}+\kappa_{AIIP}N_{^3O_2})N_{AII_g}, \tag{16}$$

$$\frac{\partial N_{CI_g}}{\partial t} = \frac{\sigma_L}{h\nu_L}I_L N_{S0}\left(\frac{k_{TCI}}{k_{TD}}\phi_{D,T}+\frac{\kappa_{OCI}}{\kappa_{ox}}\phi_{D,ox}\right) - (k_{CIP}+\kappa_{CIP}N_{^3O_2})N_{CI_g}, \tag{17}$$

$$N_P = N_{C,0} - N_{S0} - N_{AI_g} - N_{AII_g} - N_{CI_g}, \tag{18}$$

where

$$\phi_{D,S} = \phi_{SD}, \tag{19a}$$

is the quantum yield of singlet excited-state degradation,

$$\phi_{TD} = \frac{k_{TD}}{k_{TS}+k_{TD}+\kappa_{TO}N_{^3O_2}}, \tag{19b}$$

is the quantum yield of direct photo-degradation of the triplet state,

$$\phi_{D,T} = \phi_T\phi_{TD}, \tag{19c}$$

is the quantum yield of triplet excited-state degradation,

$$\phi_{D,ox} = \phi_T\frac{\kappa_{ox}\kappa_{TO}}{(k_{O13}+\kappa_{ox}N_{S0})(k_{TS}+k_{TD}+\kappa_{TO}N_{^3O_2})} \times N_{^3O_2}N_{S0}, \tag{19d}$$

$$\phi_{D,ox} \approx \phi_T\frac{\kappa_{ox}}{k_{O13}}\frac{\kappa_{TO}N_{^3O_2}}{k_{TS}+\kappa_{TO}N_{^3O_2}}N_{S0}, \tag{19e}$$

$$\phi_{D,ox} = \phi_{D,ox,0}\frac{N_{S0}}{N_{C,0}} \tag{19f}$$

is the oxidative contribution to the quantum yield of photo-degradation. If the triplet relaxation rate due to singlet-oxygen generation, $\kappa_{TO}N_{^3O_2}$, dominates over the direct triplet singlet relaxation rate, k_{TS}, then $\phi_{D,ox}$ (Eq. (19e)) reduces further to

$$\phi_{D,ox} \approx \phi_T\frac{\kappa_{ox}}{k_{O13}}N_{S0}. \tag{19g}$$

The total quantum yield of photo-degradation is

$$\phi_D = \phi_{D,S}+\phi_{D,T}+\phi_{D,ox} = \phi_{D,S}+\phi_{D,T}+\phi_{D,ox,0}\frac{N_{S0}}{N_{C,0}}. \tag{19h}$$

The initial total quantum yield of photo-degradation is

$$\phi_{D,0} = \phi_{D,S} + \phi_{D,T} + \phi_{D,ox,0}. \quad (19i)$$

$\phi_{D,0}$ depends on the concentration of triplet oxygen, $^3O_2$, and on the initial concentration of Bchlc, $N_{C,0}$. The approximation in Eq. (19e) is valid since it is $k_{O13} \gg \kappa_{ox} N_{S0}$ and $k_{TD} \ll k_{TS} + \kappa_{TO} N_{^3O_2}$. It should be noted that $\phi_{D,ox}$ is proportional to the number density, N_{S0}, of Bchlc and therefore becomes smaller as Bchlc degrades. $\phi_{D,ox,0}$ is the initial oxidative quantum yield of photo-degradation. At high oxygen concentration it saturates towards $\phi_{D,ox,0} \rightarrow \phi_T(\kappa_{ox}/k_{O13})N_{C,0}$. It should also be noted that $\phi_{D,T}$ (Eq. (19c)) depends on the triplet oxygen content of the solution, since ϕ_{TD} depends on $N_{^3O_2}$ (Eq. (19b)). The triplet lifetime of Bchlc, $\tau_T = (k_{TS} + k_{TD}\kappa_{TO}N_{^3O_2})^{-1}$, is shortened by triplet-oxygen quenching [22] while the direct triplet degradation rate, k_{TD}, is independent of the oxygen content ($\phi_{D,T}$ becomes smaller with rising triplet-oxygen concentration). The quantum yield, $\phi_{D,S}$, of singlet excited-state photo-degradation is thought to be negligibly small compared to the quantum yield, $\phi_{D,T}$, of triplet-state photo-degradation because of the high quantum yield of triplet formation ($\phi_T \approx 0.65$ [22]) and the short singlet-state lifetime compared to the triplet-state lifetime.

The fraction of photo-degradation due to singlet-state excitation is $\chi_S = \phi_{D,S}/\phi_D$, the fraction due to triplet-state excitation is $\chi_T = \phi_{D,T}/\phi_D$, and the fraction due to photo-oxidation is $\chi_{ox} = \phi_{D,ox}/\phi_D$ ($1 = \chi_S + \chi_T + \chi_{ox}$).

The simulations in Fig. 4 for the three specific excitation wavelengths, $\lambda_L = 672$, 632.8, and 428 nm (air-saturated samples), and in Fig. 9 for $\lambda_L = 672$ nm (de-aerated sample) are carried out by assuming that only one photoproduct, indicated by subscript j, is dominant at the considered wavelength. With this approximation the equation system [9,14–18] for the simulations simplifies to

$$\frac{\partial N_{S0}}{\partial t} = -\frac{\sigma_L}{h\nu_L} I_L N_{S0} \phi_D, \quad (20)$$

$$\frac{\partial N_j}{\partial t} = \frac{\sigma_L}{h\nu_L} I_L N_{S0} \phi_D \beta_j - (k_{jP} + \kappa_{jP} N_{^3O_2}) N_j, \quad (21)$$

$$\frac{\partial I_L}{\partial z} = -(\sigma_L N_{S0} + \sigma_{L,j} N_j) I_L - \alpha_{L,res} I_L. \quad (22)$$

where β_j is the branching ratio of Bchlc molecules degrading to j [$\beta_j = \kappa_{Oj}/(\kappa_{OP} + \kappa_{OAI} + \kappa_{OAII} + \kappa_{OCI})$].

The theoretical curves in Figs. 4 and 9 are calculated by use of Eqs. (20)–(22) and the parameters, $\phi_{D,0}$, $\chi_S = 0$, χ_T, χ_{ox}, $\kappa_{jP} N_{^3O_2}$, and $\sigma_{L,j}\beta_j$, listed in the figure captions. A discussion is given below.

$$^1\text{Bchlc}\ (N_{S0}) + h\nu_L \xrightarrow{\sigma_L} {}^1\text{Bchlc}^*\ (N_{S1})$$

$$^1\text{Bchlc}^*\ (N_{S1}) \xrightarrow{\phi_D} \text{D}\ (N_D)$$

Scheme 3. Photo-excitation and degradation dynamics of Bchlc in intact cells.

4.2. Photo-stability of bacteriochlorophyll c in intact cell suspensions

The Bchlc in the intact cells turned out to be very stable. There the exited-state lifetime is short because of excitonic energy transfer to the reaction center, and the singlet oxygen is quenched by the carotenoids [1,42]. The photo-degradation may be described by the simple Scheme 3.

The photo-degradation dynamics is governed by

$$\frac{\partial N_{S0}}{\partial t} = -\frac{\sigma_L}{h\nu_L} I_L N_{S0} + (1 - \phi_D)\frac{N_{S1}}{\tau_F}, \quad (23)$$

$$\frac{\partial N_{S1}}{\partial t} = \frac{\sigma_L}{h\nu_L} I_L N_{S0} - \frac{N_{S1}}{\tau_F}, \quad (24)$$

$$\frac{\partial N_D}{\partial t} = \phi_T \frac{N_{S1}}{\tau_F}, \quad (25)$$

$$\frac{\partial I_L}{\partial z} = -\sigma_L N_{S0} I_L. \quad (26)$$

The steady-state condition of Eq. (13a) reduces the Eqs. (23)–(26) to

$$\frac{\partial N_{S0}}{\partial t} = -\frac{\partial N_D}{\partial t} = -\frac{\sigma_L}{h\nu_L} I_L N_{S0} \phi_D, \quad (27)$$

$$\frac{\partial I_L}{\partial z} = -\sigma_L N_{S0} I_L, \quad (28)$$

where ϕ_D is an effective quantum yield of photo-degradation, and any photoproduct absorption at the excitation wavelength is neglected.

The curves in Fig. 3 for the intact cells are calculated by use of Eqs. (27) and (28). The best-fitting quantum yield of photo-degradation is $\phi_D = 8 \times 10^{-7}$ for both the air-saturated sample and the anaerobic sample.

5. Discussion

Quantum yields of photo-degradation are extracted from the best fits in Fig. 4 (air-saturated solution), Fig. 9 (nitrogen-bubbled solution), and Fig. 3 (intact cells).

Bchlc in the chlorosomes of intact *Chlorobium tepidum* cells turned out to be very photo-stable both under aerobic and anaerobic conditions ($\phi_D \approx 8 \times 10^{-7}$, cycles of photo-excitation before degradation are $\phi_D^{-1} \approx 1.25 \times 10^6$). The excited-state lifetime of bacteriochlorophyll c is only in the picosecond time range since the excitation is transferred

to Bchla and to the reaction center [43,44]. The carotenoids in the chlorosomes quench Bchlc and Bchla triplets and hinder singlet-oxygen formation [45].

Bchlc molecules in the acetone–methanol–water extract from *Chlorobium tepidum* exhibit a low photo-stability in air-saturated solution ($\phi_{D,0} \approx 0.011$ at $C_{C,0} \approx 6.9 \times 10^{-6}$ mol dm^{-3} and $\lambda_L = 672$ nm).

In nitrogen-bubbled Bchlc solution the photo-stability increases approximately a factor of ten compared to the air-saturated solution ($\phi_{D,0} \approx 0.0012$ at $C_{C,0} \approx 6.9 \times 10^{-6}$ mol dm^{-3} and $\lambda_L = 672$ nm). About 90% of the molecules are degraded directly from the triplet state ($\chi_T = 0.9$) and the rest is degraded by photo-oxidation (χ_T determined by best fit of theory to experimental degradation curve in Fig. 9). The oxygen content of the nitrogen-bubbled solution was determined to be $C_{^3O_2} \approx 1 \times 10^{-5}$ mol dm^{-3} by absorption actinometry with 1,3-diphenylisobenzofuran.

The number density of triplet oxygen in air-saturated solution is estimated from solubility data of oxygen in water, methanol, and acetone given in [46] by using the relation $N_{^3O_2,\text{mixture}} = \sum_i x_i N_{^3O_2,i}$, where x_i is the mole-fraction of component i in the solvent mixture ($C_{^3O_2} \approx 2.77 \times 10^{-4}$ mol dm^{-3} for water, 2×10^{-3} mol dm^{-3} for methanol, 2.25×10^{-3} mol dm^{-3} for acetone [46]). A value of $C_{^3O_2} \approx 2 \times 10^{-3}$ mol dm^{-3} is obtained (see Table 1).

In Fig. 8 the intermediate photoproduct degradation in the dark after light exposure is shown for an air-saturated Bchlc solution. This dark degradation is dominated by bimolecular catalytic action of the dissolved oxygen, i.e. the decay times are given by $\tau_j \approx (k_{jP} C_{^3O_2})^{-1}$. The extracted bimolecular degradation rate constants, κ_{AIP}, κ_{AIIP}, and κ_{CIP}, are listed in Table 1.

The intermediate photoproduct degradation in the dark of N_2-bubbled samples is shown in Fig. 12. There the dark degradation is thought to be due to the intrinsic thermal instability of the intermediates. The obtained decay rates, k_{AIP}, k_{AIIP}, and k_{CIP}, are listed in Table 1.

The initial quantum yield of oxidative photo-degradation, $\phi_{D,ox,0}$ (Eq. (19f)) depends on the quantum yield of triplet formation, ϕ_T; the rate of singlet-oxygen relaxation to triplet oxygen, k_{O13}; the bimolecular oxidative degradation rate constant, κ_{ox}; the bimolecular constant of singlet-oxygen generation in the triple state, κ_{TO}; the triplet oxygen concentration, $C_{^3O_2}$; the Bchlc concentration, $C_{C,0}$; and the rate of triplet to singlet relaxation, k_{TS}. Values for ϕ_T and κ_{TO} are taken from [22] and listed in Table 1. $k_{O13} = 1/\tau_{^1O_2}$ is estimated from the singlet-oxygen lifetimes in water, methanol, and acetone given in [40] by using the relation $k_{O13,\text{mixture}} = \sum_i x_i k_{O13,i}$ ($\tau_{^1O_2} = 2\,\mu$s for water, 7 μs for methanol, and 26 μs for acetone). A value of $k_{O13} = 1.05 \times 10^5$ s^{-1} is obtained.

The unknown parameters, κ_{ox} and k_{TS} are calculated from the measured quantum yields of photo-oxidation, $\phi_{D,ox,0}$, at air-saturated conditions and N_2-bubbled conditions. For the air-saturated samples the photo-degradation is strongly governed by photo-oxidation, since under de-aerated conditions the photo-degradation reduces a factor of ten despite the enlarged triplet-state lifetime. In a first approximation κ_{ox} is obtained from Eq. (19g) for the air-saturated situation using $\phi_{D,ox,0} \approx \phi_{D,0} = 0.011$ (Fig. 4a) and parameters from Table 1 giving $\kappa_{ox}^{(1)} \approx 2.6 \times 10^8$ m^3 mol^{-1} s^{-1}. Now k_{TS} is estimated from the photo-oxidation under de-aerated conditions by use of Eq. (19e). There it is $\phi_{D,ox} \approx 0.1\phi_{D,0} = 1.2 \times 10^{-4}$ (Fig. 9) and the triplet-singlet relaxation rate turns out to be $k_{TS} \approx 1.8 \times 10^6$ s^{-1}. In a second approximation this value is entered to Eq. (19e) for the air-saturated situation (Fig. 4a) giving $\kappa_{ox}^{(2)} \approx 3.7 \times 10^8$ dm^3 mol^{-1} s^{-1} $\approx \kappa_{ox}$.

The triplet lifetime due to triplet-singlet relaxation, $\tau_{TS} = k_{TS}^{-1} \approx 560$ ns, is rather short. This short lifetime is thought to be due to triplet-state quenching by the carotenoids present in our Bchlc extract from *Chlorobium tepidum* in acetone–methanol–water solution. The large triplet-singlet relaxation rate is responsible for the reduction of photo-degradation by nitrogen bubbling. Otherwise, ($k_{TS} \to 0$), $\phi_{D,ox}$ would rise to constant value (Eq. (19e), independent of triplet-oxygen concentration), and $\phi_{D,T}$ would approach ϕ_T (Eqs. (19b) and (19c)) with decreasing $C_{^3O_2}$ leading to an overall rise of ϕ_D with decreasing $C_{^3O_2}$.

The rate of direct triplet-state degradation of Bchlc in solution, k_{TD}, is obtained by application of Eq. (19b) for the triplet-state photo-degradation of N_2-bubbled solution ($\phi_{D,T} \approx 0.9\phi_{D,0} \approx \phi_T k_{TD}/k_{TS}$). The obtained value is $k_{TD} \approx 3 \times 10^3$ s^{-1}. It is listed in Table 1.

For air-saturated solution, the application of $k_{TD} = 3 \times 10^{-3}$ s^{-1}, $k_{TS} = 1.8 \times 10^6$ s^{-1}, $\kappa_{TO} = 2 \times 10^9$ dm^3 mol^{-1} s^{-1}, $C_{^3O_2} = 2 \times 10^{-3}$ mol dm^{-3}, and $\phi_T = 0.65$ to Eq. (19b) and (19c) gives $\phi_{D,T} = 2.2 \times 10^{-4}$, while $\phi_{D,0} = 0.011$ at $\lambda_L = 672$ nm. The fraction of direct photo-degradation from the triplet state comes out to be $\chi_T = 0.02$, and the fraction of degradation due to photo-oxidation is found to be $\chi_{ox} = 1 - \chi_T = 0.98$.

The branching ratios, $\beta_j = \kappa_{Oj}/\kappa_{ox}$, of the Bchlc degradation to the intermediate photoproducts j (j = AI, AII, CI for air-saturated solutions, j = AI′, AII′, CI′ for nitrogen-bubbled solutions) are estimated from the ratios of photoproduct-absorption-increase to Bchlc-absorption-decrease at the peak absorption wavelengths within a certain exposure time period according to $\beta_j = \Delta\alpha_j(\lambda_{j,\max})/\Delta\alpha_{Bchlc}(\lambda_{Bchlc,\max})$. Thereby it is assumed that the intermediate photoproducts (bacteriochlorophyll derivatives) have the same oscillator strength and spectral halfwidths as Bchlc. The branching ratio for Bchlc-O_2 generation with subsequent ring-opening to linear tetrapyrroles is approximately given by $\beta_P = 1 - \beta_{AI} - \beta_{AII} - \beta_{CI}$ for the air-saturated solutions and by $\beta_P = 1 - \beta_{AI'} - \beta_{AII'} - \beta_{CI'}$ for the nitrogen-bubbled solutions. The resulting values are collected in Table 1.

Table 1
Relevant parameters for photo-degradation of Bacteriochlorophyll c from *Chlorobium tepidum* extract in acetone–methanol–water mixture (7:2:1) at room temperature

Parameter	Air-saturated solutions	Comments	Parameter	Nitrogen-bubbled solution	Comments
$C_{^3O_2}$ (mol dm^{-3})	$\approx 2 \times 10^{-3}$	Estimated from data in [46]	$C_{^3O_2}$ (mol dm^{-3})	$\approx 1 \times 10^{-5}$	Own DPBF actionometry
$\phi_{D,0}$ at $\lambda_L = 672$ nm	0.011 ± 0.001	Fig. 4a, $N_{C,0} = 4.2 \times 10^{15}$ cm^{-3}	$\phi_{D,0}$ at $\lambda_L = 672$ nm	$\approx 1.2 \times 10^{-3}$	Fig. 9
$\phi_{D,0}$ at $\lambda_L = 632.8$ nm	0.018 ± 0.002	Fig. 4b, $N_{C,0} = 4.9 \times 10^{15}$ cm^{-3}			
$\phi_{D,0}$ at $\lambda_L = 428$ nm	0.020 ± 0.002	Fig. 4c, $N_{C,0} = 4.65 \times 10^{15}$ cm^{-3}			
χ_T at $\lambda_L = 672$ nm	0.02	$\chi_T = \phi_{D,T}/\phi_{D,0}$	χ_T at $\lambda_L = 672$ nm	≈ 0.9	Fig. 9, $\chi_T = \phi_{D,T}/\phi_{D,0}$
χ_{ox} at $\lambda_L = 672$ nm	0.98	$\chi_{ox} = \phi_{D,ox,0}/\phi_{D,0}$	χ_{ox} at $\lambda_L = 672$ nm	≈ 0.1	Fig. 9, $\chi_{ox} = \phi_{D,ox,0}/\phi_{D,0}$
κ_{AIP} (dm^3 mol^{-1} s^{-1})	1.63×10^{-1}	Fig. 8a and $\tau = (\kappa_{AIP} N_{^3O_2})^{-1}$	$k_{AI'P}$ (s^{-1})	9.2×10^{-6}	Fig. 12, decay at 760 nm
κ_{AIIP} (dm^3 mol^{-1} s^{-1})	7.04×10^{-2}	Fig. 8b and $\tau = (\kappa_{AIIP} N_{^3O_2})^{-1}$	$k_{AII'P}$ (s^{-1})	9.5×10^{-6}	Fig. 12, decay at 730 nm
κ_{CIP} (dm^3 mol^{-1} s^{-1})	6.59×10^{-2}	Fig. 8c and $\tau = (\kappa_{CIP} N_{^3O_2})^{-1}$	$k_{CI'P}$ (s^{-1})	1.31×10^{-5}	Fig. 12, decay at 690 nm
k_{O13} (s^{-1})	$\approx 1.05 \times 10^5$	Estimated from data in [40]			
ϕ_T	≈ 0.65	From [22]			
κ_{ox} (dm^3 mol^{-1} s^{-1}) at $\lambda_L = 672$ nm	3.7×10^8	Eq. (19e), see text			
β_{AI} at $\lambda_L = 672$ nm	≈ 0.21	Fig. 5, $\beta_{AI} = \Delta\alpha(760\text{ nm})/\Delta\alpha(665\text{ nm})$	$\beta_{AI'}$	≈ 0.17	Fig. 10, $\beta_{AI'} = \Delta\alpha$ (765 nm)/$\Delta\alpha$ (665 nm)
β_{AII} at $\lambda_L = 672$ nm	≈ 0.19	Fig. 5, $\beta_{AII} = \Delta\alpha(730\text{ nm})/\Delta\alpha(665\text{ nm})$	$\beta_{AII'}$	≈ 0.12	Fig. 10, $\beta_{AI'} = \Delta\alpha$ (735 nm)/$\Delta\alpha$ (665 nm)
β_{CI} at $\lambda_L = 672$ nm	≈ 0.18	Fig. 5, $\beta_{CI} = \Delta\alpha(690\text{ nm})/\Delta\alpha(665\text{ nm})$	$\beta_{CI'}$	≈ 0.12	Fig. 10, $\beta_{CI'} = \Delta\alpha$ (685 nm)/$\Delta\alpha$ (665 nm)
β_P at $\lambda_L = 672$ nm	≈ 0.42	$\beta_P \approx 1 - (\beta_{AI} + \beta_{AII} + \beta_{CI})$	β_P	≈ 0.56	$\beta_P \approx 1 - (\beta_{AI'} + \beta_{AII'} + \beta_{CI'})$
κ_{TO} (dm^3 mol^{-1} s^{-1})	$\approx 2 \times 10^9$	From [22]			
τ_T (ns)	≈ 250	$\tau_T \approx (\kappa_{TO} C_{^3O_2})^{-1}$	τ_T (ns)	≈ 560	$\tau_T = k_{TS}^{-1}$
			k_{TS} (s^{-1})	$\approx 1.8 \times 10^6$	Eq. (19e), see text
			k_{TD} (s^{-1})	$\approx 3 \times 10^3$	Eq. (19b)

6. Conclusions

The photo-stability of Bchlc in intact cells and in an acetone–methanol–water extract of *Chlorobium tepidum* was studied under anaerobic and aerobic conditions. Quantitative initial quantum yields of photo-degradation have been determined and the degradation path has been analyzed. A rate equation system for the degradation dynamics has been developed, and has been reduced to special considerations of parameter extraction.

The photo-stability of Bchlc in the chlorosomes of intact cells has been found to be very high. The high photo-stability is thought to be due the short excited-state lifetime in the chlorosomes and the Bchlc protection in the chlorosomes.

The photo-stability of single Bchlc molecules from a *Chlorobium tepidum* extract in an acetone–methanol–water solution turned out to be low under air-saturated conditions and moderate under de-aerated conditions. In air-saturated solution the photo-degradation is determined by photo-oxidation. Photo-excitation of single Bchlc molecules in air-saturated solution leads to singlet-oxygen generation, and the generated singlet oxygen causes intermediate photoproduct formation and subsequent degradation to linear tetrapyrroles.

In N_2-bubbled de-aerated Bchlc extracts from *Chlorobium tepidum* the photo-degradation is dominated by direct triplet-state photo-degradation. The short triplet-state lifetime caused by carotenoid-triplet-state-quenching is thought to be responsible for the increase in photo-stability by triplet-oxygen reduction.

In carotenoid-free Bchlc solutions the rate constants of oxidative degradation, κ_{ox} and direct triplet-state degradation, k_{TD}, are expected to be unchanged. The quantum yield of photo-degradation of air-saturated samples should be nearly the same as in the carotenoid-containing samples studied here. For the carotenoid-free de-aerated Bchlc solutions the photo-stability is expected to be less than in our carotenoid-containing samples because of the enlarged triplet-state lifetime.

The presented method and analysis of photo-degradation may be generally applied to photo-degradation studies of bacteriochlorophylls, chlorophylls, and other molecules.

Acknowledgements

We thank Monika Kammerer for *Chlorobium tepidum* cultivation. We thank the Deutsche Forschungsgemeinschaft (DFG) for support in the Graduate College, GK640/1, “Sensory photoreceptors in natural and artificial systems”, which enabled this collaborative work.

References

[1] R.E. Blankenship, J.M. Olson, M. Miller, in: R.E. Blankenship, M.T. Madigan, C.E. Bauer (Eds.), Annoxygenic Photosynthetic Bacteria, Kluwer Academic Publishers, Dordrecht, The Netherlands, 1995, p. 399.
[2] J.M. Olson, Photochem. Photobiol. 67 (1998) 61.
[3] J.A. Eisen, K.E. Nelson, I.T. Paulsen, J.F. Heidelberg, M. Wu, R.J. Dodson, R. Deboy, M.L. Gwinn, W.C. Nelson, D.H. Haft, E.K. Hickey, J.D. Peterson, A.S. Durkin, J.L. Kolonay, F. Yang, I. Holt, L.A. Umayam, T. Mason, M. Brenner, T.P. Shea, D. Parksey, W.C. Nierman, T.V. Feldblyum, C.L. Hansen, M.B. Craven, D. Radune, J. Vamathevan, H. Khouri, O. White, T.M. Gruber, K.A. Ketchum, J.C. Venter, H. Tettelin, D.A. Bryant, C.M. Fraser, PNAS 99 (2002) 9509.
[4] N.-U. Frigaard, A.G.M. Chew, H. Li, J.A. Maresca, D.A. Bryant, Photosynth. Res. 78 (2003) 93.
[5] C.M. Borrego, P.D. Gerola, M. Miller, R.P. Cox, Photsynth. Res. 59 (1999) 159.
[6] J. Oelze, J.R. Golecki, in: R.E. Blankenship, M.T. Madigan, C.E. Bauer (Eds.), Annoxygenic Photosynthetic Bacteria, Kluwer Academic Publishers, Dordrecht, The Netherlands, 1995, p. 259.
[7] C. Hager-Braun, R. Zimmermann, G. Hauska, in: G.A. Peschek W. Löffelhardt, G. Schmetterer (Eds.), The Phototrophic Prokaryotes, Kluwer Academic Publishers, New York, 1999, p. 169.
[8] G. Hauska, T. Schoedl, H. Remigy, G. Tsiotis, Biochim. Biophys. Acta 1507 (2001) 260.
[9] D.R. Buck, W.S. Struve, Photosynth. Res. 48 (1996) 367.
[10] V.I. Prokhorrenko, D.B. Steensgaard, A.R. Holzwarth, Biophys. J. 79 (2000) 2105.
[11] J. Oelze, Methods Microbiol. 18 (1985) 257.
[12] H. Scheer, in: H. Scheer (Ed.), Chlorophylls, CRC Press, Boca Raton, 1991, p. 3.
[13] P.H. Hynninen, in: H. Scheer (Ed.), Chlorophylls, CRC Press, Boca Raton, 1991, p. 145.
[14] W.R. Richards, in: M. Goodfellow, A.G. O’Donnell (Eds.), Chemical Methods in Prokaryotic Systematics, Wiley, New York, 1994, p. 345.
[15] R. Bonnett, in: D. Dolphin (Ed.), The Porphyrins, vol. 1, Academic Press, New York, 1978, p. 1.
[16] G.B. Moss, Pure Appl. Chem. 59 (1987) 779.
[17] R. Bonnett, G. Martínez, Tetrahedron 57 (2001) 9513.
[18] G.W. Kenner, J. Rimmer, K.M. Smith, J.F. Unsworth, J. Chem. Soc., Perkin Trans. 1 (9) (1978) 845.
[19] N. Risch, A. Schormann, H. Brockmann, Tetrahedron Lett. 25 (1984) 5993.
[20] S.B. Brown, K.M. Smith, G.M.F. Bisset, R.F. Troxler, J. Biol. Chem. 255 (1980) 8063.
[21] R.F. Troxler, K.M. Smith, S.B. Brown, Tetrahedron Lett. 21 (1980) 491.
[22] A.A. Krasnovsky, P. Cheng, R.E. Blankenship, T.A. Moore, D. Gust, Photochem. Photobiol. 52 (1993) 324.
[23] A.A. Krasnovsky, Photochem. Photobiol. 29 (1979) 29.
[24] A.A. Krasnovsky, Biophysics 39 (1994) 197.
[25] T.M. Wahlund, C.R. Woese, R.W. Castenholz, M.T. Madigan, Arch. Microbiol. 150 (1991) 81.
[26] N.U. Frigaard, S. Takaichi, M. Hirota, K. Shimada, K. Matsuura, Arch. Microbiol. 167 (1997) 343.
[27] S. Takaichi, Z.-Y. Wang, M. Umetsu, T. Nozawa, K. Shimada, M.T. Madigan, Arch. Microbiol. 168 (1997) 270.
[28] N.-U. Frigaard, K.L. Larsen, R.P. Cox, FEMS Microbiol. Ecol. 20 (1996) 69.
[29] T. Tsuji, S. Tahaichi, K. Matsuura, K. Shimada, in: P. Mathis (Ed.), Photosynthesis: From Light to Biosphere, vol. 3, Kluwer Academic Publishers, Dordrecht, The Netherlands, 1995, p. 99.
[30] G. Britton, in: G. Britton, S. Liaaen-Jensen, H.P. Pfander (Eds.), Carotenoids: Spectroscopy, vol. 1b, Birkhäuser, Basel, 1995, p. 13.
[31] H. Holo, M. Broch-Due, J.G. Ormerod, Arch. Microbiol. 143 (1985) 94.
[32] K. Schmidt, A. Connor, G. Britton, in: M. Goodfellow, A.G. O’Donnell (Eds.), Chemical Methods in Prokaryotic Systematics, Wiley, New York, 1994, p. 403.
[33] R.Y. Stanier, J.H.C. Smith, Biochim. Biophys. Acta 41 (1960) 478.

[34] B.K. Pierson, R.W. Castenholz, Arch. Microbiol. 100 (1974) 283.
[35] W. Jürgens, H. Brockmann, Z. Naturforsch. 84b (1979) 1026.
[36] R.H. Young, D.R. Brewer, in: R. Ranby, J.F. Rabek (Eds.), Singlet Oxygen. Reactions with Organic Compounds and Polymers, Wiley, Chichester, 1978, p. 36.
[37] A. Granzhan, A. Penzkofer, G. Hauska, to be published.
[38] W. Holzer, M. Mauerer, A. Penzkofer, R.-M. Szeimies, C. Abels, M. Landthaler, W. Bäumler, J. Photochem. Photobiol. B: Biol. 47 (1998) 155.
[39] D.C. Brune, R.E. Blankenship, G.R. Seely, Photochem. Photobiol. 47 (1988) 759.
[40] P.B. Merkel, D.R. Kearns, J. Am. Chem. Soc. 97 (1972) 1029.
[41] C. Schweitzer, R. Schmidt, Chem. Rev. 103 (2003) 165.
[42] H. van Amerongen, L. Valkunas, R. van Grondelle, Photosynthetic Excitons, World Scientific, Singapore, 2000.
[43] H. Oh-oka, S. Kamei, H. Matsubara, S. Lin, P.I. van Noort, R.E. Blankenship, J. Phys. Chem. B 102 (1998) 8190.
[44] J. Psencik, T. Polivka, P. Nemec, J. Dian, J. Kudrna, P. Maly, J. Hala, J. Phys. Chem. A 102 (1998) 4392.
[45] T.B. Melo, N.U. Frigaard, K. Matsuura, K. Razi Naqvi, Spectrochim. Acta A 56 (2000) 2001.
[46] A. May, in: E. Lax (Ed.), D'Ans Lax. Taschenbuch für Chemiker und Physiker: Makroskopische und physikalisch-chemische Eigenschaften, vol. 1, third ed., Springer-Verlag, Berlin, 1967, pp. 1–1203.
[47] T. Nozawa, K. Ohtomo, M. Suzuki, H. Nakagawa, Y. Shiakma, Photosynth. Res. 41 (1994) 211.